CORA Cork Open Research Archive
Cartlann Taighde Oscailte Chorcaí

Title	Examining the role of electrolyte and binders in determining discharge product morphology and cycling performance of carbon cathodes in Li-O2 Batteries
Authors	Geaney, Hugh;O'Dwyer, Colm
Publication date	2015-11-04
Original Citation	Geaney, H. and O'Dwyer, C. (2016) 'Examining the Role of Electrolyte and Binders in Determining Discharge Product Morphology and Cycling Performance of Carbon Cathodes in Li-O2 Batteries', Journal of The Electrochemical Society, 163(2), pp. A43-A49. doi: 10.1149/2.1011514jes
Type of publication	Article (peer-reviewed)
Link to publisher's version	http://jes.ecsdl.org/content/163/2/A43.full.pdf+html - 10.1149/2.1011514jes
Rights	© The Author(s) 2015. Published by ECS. This is an open access article distributed under the terms of the Creative Commons Attribution 4.0 License (CC BY, http://creativecommons.org/licenses/by/4.0/), which permits unrestricted reuse of the work in any medium, provided the original work is properly cited. - http://creativecommons.org/licenses/by/4.0/
Download date	2024-10-12 04:28:46
Item downloaded from	https://hdl.handle.net/10468/6052

UCC
University College Cork, Ireland
Coláiste na hOllscoile Corcaigh

Examining the Role of Electrolyte and Binders in Determining Discharge Product Morphology and Cycling Performance of Carbon Cathodes in Li-O_2 Batteries

Hugh Geaney[a,b] and Colm O'Dwyer[a,b,*,z]

[a]*Department of Chemistry, University College Cork, Cork, T12 YN60, Ireland*
[b]*Micro-Nano Systems Centre, Tyndall National Institute, Lee Maltings, Cork, T12 R5CP, Ireland*

In this report we examine the influence of electrode binder and electrolyte solvent on the electrochemical response of carbon based Li-O_2 battery cathodes. Much higher discharge capacities were noted for cathodes discharged in DMSO compared to TEGDME. The increased capacities were related to the large spherical discharge products formed in DMSO. Characteristic toroids which have been noted in TEGDME electrolytes previously were not observed due to the low water content of the electrolyte. Linear voltage sweeps were used to investigate ORR in both of the solvents for each of the binder systems (PVDF, PVP, PEO and PTFE) and related to the Li_2O_2 formed on the cathode surfaces. Galvanostatic tests were also conducted in air as a comparison with the pure O_2 environment typically used for Li-O_2 battery testing. Interestingly, tests for the two electrolytes showed opposite trends in terms of discharge capacity values with capacities increased in TEGDME (compared to those seen in O_2) and decreased in DMSO. The report highlights the key roles of electrolyte and cathode composition in determining the stability of Li-O_2 batteries and highlights the importance of identifying more stable electrolyte/cathode pairings.
© The Author(s) 2015. Published by ECS. This is an open access article distributed under the terms of the Creative Commons Attribution 4.0 License (CC BY, http://creativecommons.org/licenses/by/4.0/), which permits unrestricted reuse of the work in any medium, provided the original work is properly cited. [DOI: 10.1149/2.1011514jes] All rights reserved.

Manuscript submitted August 28, 2015; revised manuscript received October 2, 2015. Published November 4, 2015.

Li-O_2 batteries are an exciting class of energy storage devices with exceptional theoretical capacities which could facilitate long-range electrical vehicles if fully optimized systems are realized.[1–5] Energy storage in Li-O_2 batteries proceeds *via* different mechanisms to those associated with conventional Li-ion batteries, necessitating detailed studies into the fundamental processes associated with discharge and charge.[6–8] It has been shown in a number of studies that the energy storage mechanism for Li-O_2 batteries involves the reversible formation/decomposition of Li_2O_2 upon discharge and charge respectively.[9–13] While the O_2 required to form Li_2O_2 during discharge can theoretically be provided from ambient air, the majority of systems investigated to date have used pure O_2 to avoid unwanted side-reactions due to the ingress of atmospheric CO_2 and H_2O.[14,15] The formation of parasitic by-products in Li-O_2 batteries (which have been found to form extensively on charging due to cathode and electrolyte instabilities) is a major hurdle to their widespread implementation.[16,17]

The nature of Li_2O_2 (i.e morphology, crystallinity, size and location on the cathode) formed during discharge, and its impact on capacity, cycle life and charging behavior has attracted recent research interest.[18–20] A number of reports have presented the formation of Li_2O_2 toroids on cathode surfaces during discharge in a variety of cathode/electrolyte systems.[7,8,12,19,21–25] Adams et al. showed that the formation of these toroids was related to the applied current for a given system (TEGDME/LiTFSI electrolyte and Super P carbon cathode).[26] Their results suggested that low applied currents tend to favor the formation of large crystalline Li_2O_2 toroids on the cathode surface with a change to quasi- amorphous Li_2O_2 films at higher applied currents. It was also stated that the toroids were much more difficult to decompose during charging than the thin films, suggesting that the nature of the Li_2O_2 formed during discharge plays a key role in determining rechargeability (a key issue for Li-O_2 batteries). Aetukuri et al. examined Li_2O_2 toroid formation as a function of electrolyte composition and H_2O content on different cathodes.[21] They found that electrolytes with high Gutman donor and acceptor numbers (DN and AN respectively) stabilize the solution mediated formation of Li_2O_2 toroids. In their study, it was found that added H_2O (as a high AN compound) can markedly increase toroid formation within a given electrolyte with their results suggesting that anhydrous dimethoxyethane (DME) does not support the formation of Li_2O_2 toroids. While the presence of H_2O aids toroid formation (which leads to higher discharge capacities) it may also cause the formation of parasitic by-products at the cathode or degrade the Li anode which severely hampers cycle life.[27] Ideally, future electrolyte solvents should possess high AN or DN to facilitate toroid formation and maximize discharge capacity without exacerbating by-product formation.[28,29]

The search for more stable electrolyte and cathode pairings for Li-O_2 batteries has become a critical area of research and will likely determine the long term prospects of the Li-O_2 system.[30,31] To date, the pursuit of sufficiently stable electrolytes (i.e. an electrolyte that would allow for hundreds of discharge/charge cycles over extended periods of time at full depth of discharge) has led to incremental improvements. It has been conclusively shown that carbonate based electrolytes are not suitable for rechargeable systems due to the rapid accumulation of carbonate based species on the cathode.[32] Ether based electrolytes (e.g. tetraethylene glycol dimethyl ether (TEGDME) and DME) have shown improved stability compared to carbonates but are still prone to decomposition on charging.[33–35] Dimethyl sulfoxide (DMSO)[9,10,36,37] and sulfolane[23] based electrolytes have also attracted attention with these studies often presenting larger discharge capacities and enhanced rechargeabililty compared to TEGDME based electrolytes. However, Younesi et al. and Kwabi et al. have recently shown that upon long term exposure of Li_2O_2 to DMSO, the discharge product is unstable and is converted into LiOH, casting doubt over the long term practicality of DMSO as a Li-O_2 electrolyte.[38,39] Despite these issues, ethers and DMSO/sulfolane are useful electrolyte systems to study the fundamental processes associated with discharge and charge and as a means of understanding the formation of Li_2O_2 on Li-O_2 battery cathodes.

A major issue with Li-O_2 battery research is the sensitivity of the electrochemical response to minute changes in a wide range of parameters. This response has been shown to vary depending on an increasingly substantial list of parameters including: the O_2 pressure and purity in the system,[14,40,41] operating temperature,[42–44] electrolyte composition (with the H_2O content of particular importance),[27,45–52] carbon type,[53–56] type of binder used,[57–59] presence of an electrocatalyst,[8,60–62] depth of discharge,[63] applied current,[7] mass loading[64] etc. Whilst all of these parameters influence the discharge voltage and ultimate discharge capacity, their impact in terms of the charging overpotential and overall charging response are particularly important. This is the case because a number of reports conclude the efficacy of 'novel' electrocatalytic material based on a decrease in charging overpotential (and/or increased charge

*Electrochemical Society Active Member.
zE-mail: c.odwyer@ucc.ie

Downloaded on 2015-11-05 to IP 143.239.221.132 address. Redistribution subject to ECS terms of use (see ecsdl.org/site/terms_use) unless CC License in place (see abstract).

capacity) compared to control samples. This factor alone does not take into account the possibility of parasitic side reactions during charging or the influence of the catalyst material on the initial formation of discharge products. As a result, judging electrocatalysis based solely on overpotential reduction is overly simplistic and true electrocatalysis should be verified using a combination of analytical methods such as idiometric titrations and DEMS analysis.[13,65,66]

In this report we investigated the formation of Li_2O_2 and cycling performance of Super P carbon based cathodes within TEGDME and DMSO based electrolytes and for four different cathode binders (PVDF, PTFE, PEO and PVP). The morphology of Li_2O_2 formed within each cathode system was found to differ for each electrolyte and was strongly linked to the water content of the electrolyte and applied current. Of the two electrolytes, DMSO showed the best cycling behavior and TEGDME based electrolytes exhibited poor rechargeabililty. Tests were also conducted in air to show that parasitic side reactions can manifest as 'improved' electrochemistry (i.e. a lowering of overpotential and improved rechargeability). The study highlights the importance of electrolyte choice in determining performance for a given cathode system while also illustrating the electrolyte dependent formation of Li_2O_2 on carbon cathodes.

Experimental

Materials.— LiTFSI (99.95%), TEGDME (≥ 99%), anhydrous DMSO (≥ 99%) were purchased from Sigma Aldrich. LiTFSi was dried under vacuum at 80°C overnight prior to use. TEGDME and DMSO were dried using freshly activated 4 Å molecular sieves. Li chips were purchased from MTI. Poly(vinylidene fluoride) ((PVDF) average Mw ∼534,000), Polyvinylpyrrolidone ((PVP) average Mw ∼29,000), Polytetrafluoroethylene ((PTFE) preparation 60 wt% dispersion in H_2O) were purchased from Sigma Aldrich. Polyethyleneoxide (PEO) was purchased from Polymer Source Inc. (average mw 97,000).

Cathode preparation.— Cathodes were prepared by creating slurries of Super P carbon and an appropriate binder (PVDF, PEO, PVP or PTFE) in a weight ratio of 4.5:1 in NMP. The binder/carbon ratio was kept constant as the discharge capacity of Li-O_2 batteries had been shown to be strongly correlated with this ratio due to changes caused in the surface area.[67] The resultant slurries were mechanically stirred before being dip coated on stainless steel mesh current collectors (diameter 1.76 cm^2). The meshes were dried overnight at 100°C to remove the solvent and transferred immediately to a glove box. The total mass loading on each of the cathodes was 1.3 ± 0.45 mg. Example SEM images of a Super P cathode containing a PVDF binder as an example are presented in Supporting information S1.

Electrochemical testing.— Electrochemical tests were performed using an El-Cell split cell. All cells were constructed within an Ar filled glove box (O_2 and H_2O < 0.1 ppm). Given the critical role of H_2O content in determining the electrochemical response, KF (Karl Fischer) analysis was performed on the different electrolytes after preparation using a Metrohm 684 KF coulometer instrument. The water content of each electrolyte examined is explicitly stated in the text when referring to the respective electrochemical tests. The figures quoted are averages of five measurements. A sample of electrolyte was removed from the glove box in a sealed container. The KF analysis was conducted in air as rapidly as possible meaning that the actual H_2O content of the electrolyte may be slightly lower than reported. The values given are thus an upper estimate on the H_2O content. All cathodes were prepared on stainless steel mesh current collectors as described above. A glass fiber filter paper was used as separator upon which 100 µl of electrolyte was added. A Li chip (MTI) was scraped on both sides and used as the anode. The cell was tightened and removed from the glove box where it was immediately connected to an O_2 line and then purged with 0.25 bar O_2 for 60 minutes at open circuit voltage (OCV). Following this period, the O_2 flow was ceased and the oxygen inlet and outlet valves were closed. The cell was allowed to rest for another hour in this closed configuration. Electrochemical measurements were conducted using a VSP Biologic galvanostat. All galvanostatic measurements were conducted using fixed applied currents rather than currents calculated based on the mass of the cathode material. All voltages quoted are vs Li/Li^+. Linear sweep voltammetry (LSV) was conducted from open circuit potential (after 2 hour OCV period as defined above) to the lower limit of 2 V at a rate of 0.05 mV/s.

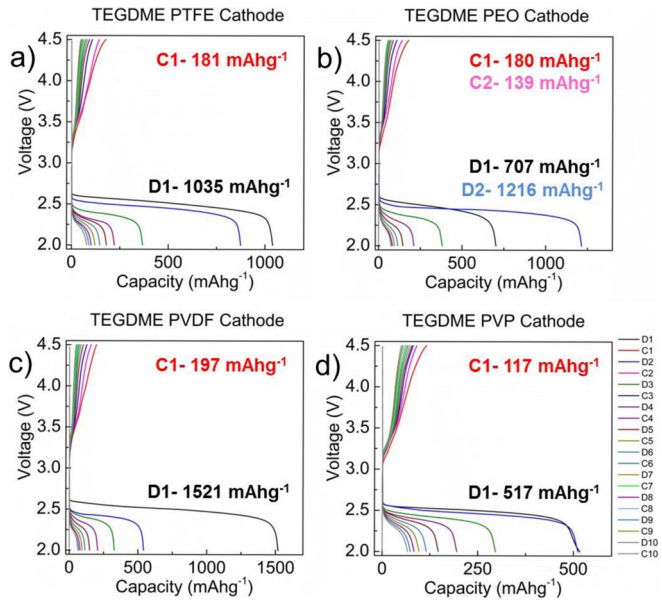

Figure 1. 10 discharge/charge cycles of Super P cathodes at a fixed current rate of 0.1 mA on a stainless steel current collector using different binders (a) PTFE binder, b) PEO binder, c) PVDF binder, d) PVP binder) in a TEGDME/LiTFSi electrolyte with a H_2O content of 207 ppm. D1 and C1 refer to discharge and charge etc.

Materials characterization.— SEM analysis was performed on an FEI Quanta 650 FEG high resolution SEM equipped with an Oxford Instruments X-MAX 20 large area Si diffused EDX detector. Images were collected at an operating voltage of 10–20 kV. All cathodes for SEM analysis were stored in an Ar filled glove box and transferred in closed containers with 0.1 ppm H_2O and O_2. Samples were loaded into the SEM as rapidly as possible (with an air exposure of <20 seconds).

Results and Discussion

Galvanostatic testing of cathodes in TEGDME and DMSO.— The binder dependent cycling performance of Super P carbon cathodes in a TEGDME/LiTFSI electrolyte with a water content of ∼200 ppm H_2O (specifically 207 ppm) was examined. The cathodes were cycled at full depth of discharge between 2 and 4.5 V (vs Li/Li^+). In Figure 1 it can be seen that the TEGDME electrodes exhibit different initial discharge capacities depending on the binder employed. These capacities decrease in the order of PVDF> PTFE> PEO >PVP. The second discharge for the PEO cathode was higher than the first discharge. Despite the fact that the initial discharge capacities were greater than 1000 $mAhg^{-1}$ for two of the four cathodes systems investigated, capacity retention was poor in all cases. All of the cathodes show extremely poor reversibility with coulombic efficiencies below 25% in each case. The 2nd discharge capacities for the four cells were all >500 $mAhg^{-1}$ but the capacities rapidly decreased after the 2nd cycle. It is clear that the performance of pure carbon cathodes in nearly anhydrous TEGDME electrolyte is not acceptable for future applications. The poor performance of these cathodes will be discussed in

Downloaded on 2015-11-05 to IP 143.239.221.132 address. Redistribution subject to ECS terms of use (see ecsdl.org/site/terms_use) unless CC License in place (see abstract).

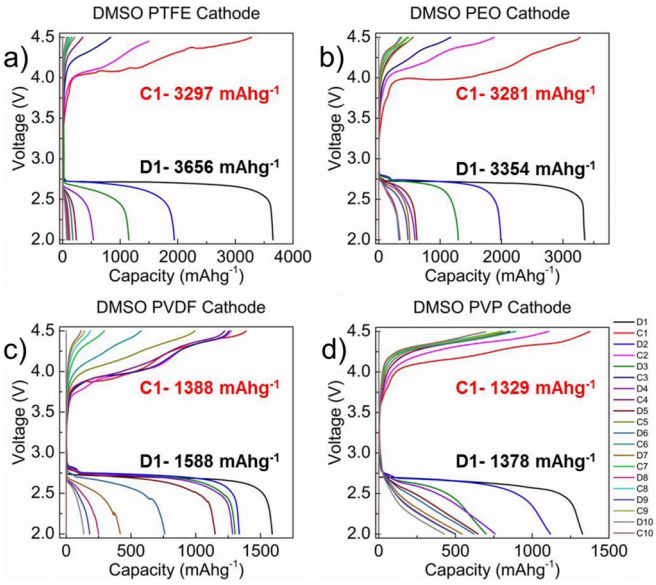

Figure 2. 10 discharge charge cycles of Super P cathodes at a fixed current rate of 0.1 mA on a stainless steel current collector using different binders (a) PTFE binder, b) PEO binder, c) PVDF binder, d) PVP binder) in a DMSO/LiTFSi electrolyte with a H_2O content of 98 ppm.

further in a later section where it will be related to the morphology of Li_2O_2 formed on the cathodes.

The cycling behavior of Super P cathodes with the same binders was investigated within a DMSO based electrolyte (Figure 2). All other parameters (cathode composition and average mass loading, cell architecture etc.) were kept fixed such that the only variable was the electrolyte solvent. The water content was also similar to the previously studied TEGDME at ≈100 ppm (98 ppm). The initial discharge capacities varied depending on the binder used in the order of PTFE>PEO>PVDF>PVP. The initial discharge for the PTFE and PEO cathodes were very high for non-catalysed planar carbon based cathodes at over 3000 $mAhg^{-1}$. In contrast to the data presented for the TEGDME electrolyte tests, the DMSO tests all showed reasonable charging behavior below 4.5 V. The onset potentials for OER increased in the order of PVDF<PVP<PEO<PTFE. The primary issue of stability for the different binders relates to the reactivity of the Li_2O_2 and its intermediates with respect to the different binders during both charge and discharge. The choice of an 'ideal' binder is a complex issue. Amanchukwa et al. recently compared the stability of different polymers in the Li-O_2 system and classed them as either stable or unstable in contact with Li_2O_2.[58] According to their results, PVP and PVDF were deemed unstable while PTFE and PEO were stable (with the latter possibly prone to some crosslinking in the presence of Li_2O_2). The unusual discharge profiles for the PVP cathode seen here after the second discharge likely indicated poorer stability of PVP compared to the other binders.

The results from the galvanostatic tests presented in Figure 1 (TEGDME) and Figure 2 (DMSO) are summarized in Figure 3. The discharge capacities for the TEGMDE tests (Figure 3a) drop quickly from the initial values and are all below 250 $mAhg^{-1}$ after just the 4th cycle. This poor discharge capacity retention can be explained by the low charge capacities (Figure 3b) and poor coulombic efficiencies (Figure 3c). In contrast, the tests conducted in DMSO show higher discharge capacities (Figure 3d) and much better rechargeability. This is reflected in the improved charge capacities (Figure 3e) and much improved coulombic efficiencies (Figure 3f). All of the coulombic efficiencies are above 60% for each of the cycles. The anomalously high coulombic efficiency values for the PVP test in DMSO suggest extensive side reactions caused by the fundamental instability of PVP in the Li-O_2 system as recently reported.[58]

To further investigate the electrochemical response for the various cathodes in the two different electrolytes outlined above, LSV tests were conducted (Figure 4). LSV has recently been used as a useful means of fingerprinting the nature of Li_2O_2 growth on Li-O_2 battery cathodes.[48] In contrast to galvanostatic tests where the discharge potential is approximately the same for different tests (i.e. the variation is typically lower than 250 mV between tests at the same current density regardless of the use of different electrolytes or electrocatalysts[20,68,69]), LSV tests conducted at slow rates (e.g. 0.5 mV/s) have shown marked differences in response. LSV run in TEGDME (nominal H_2O content 200 ppm) showed different responses for each of the cathodes (Figures 4a–4d). The total integrated area (charge) of the curves descended in the order of PTFE> PEO≈PVDF>PVP. The data was deconvoluted into two peaks; one at higher voltage (surface dominated peak shown in green) and the other at lower voltage (solution dominated peak shown in red) as previously reported.[48] The percentage contribution for each peak to the overall data is given in each plot. While it can be seen that the solution based processes dominate for the tests conducted in TEGDME, in the cases of PEO, PVDF and PVP a sizeable contribution is made to the raw data by the higher voltage, surface driven peak (30%, 20%, 23% respectively). In contrast, the DMSO tests showed a much lower contribution from surface driven processes, with the PTFE and PEO cathode showing only 3 and 4% surface processes respectively. The total integrated area for the tests in DMSO decreased in the order of PTFE>PEO>PVP>PVDF, which compares well with the discharge capacities seen in the galvanostatic tests (Figure 2). The higher discharge capacities for PTFE and PEO based cathodes in DMSO (where discharge proceeds primarily through a single discharge mechanism) correlate well with the relative stabilities of the binders as described by Amanchukwu et al.[58]

SEM analysis was used to identify the morphology of discharge products on the different carbon cathodes after linear voltage sweeps to 2 V in DMSO (Figure 5). This was used as a means of examining the differences in peak location and the magnitudes of currents between the two electrolyte systems and between different cathodes. For the cathodes discharged voltammetrically in DMSO, spherical discharge products were identified on the cathodes containing PEO (average ≈300 nm in size), PTFE (average ≈450 nm) and PVP (average ≈600 nm) with the average particle size increasing in that order. While these spherical discharge products are consistent with previous results for Li_2O_2 formed on Li-O_2 battery cathodes, we cannot rule out the formation of other side-products. This increase in particle size is also possibly reflected in a downshifting of the solution driven peak position for ORR caused by more solution mediated Li_2O_2 growth as described by Aetukuri et al.[45] Additionally, the density of discharge products on the cathodes containing PEO and PTFE (which showed almost exclusively solution driven processes in Figures 4e–4f) are much higher than that seen for PVP (which showed a larger contribution from surface processes). In contrast, the PVDF cathode showed a different discharge product morphology. This flaked discharge product is consistent with our previous observations of the discharge products formed during galvanostatic discharges of PVDF cathode within a DMSO electrolyte and is again likely linked to the formation of LiOH (and likely LiOH.H_2O) due to interactions between the PVDF and the DMSO electrolyte.[46]

SEM images of the cathodes after LVS discharges in TEGDME (Figure 6) were obviously different to those seen for the DMSO cathodes in Figure 5. In contrast to the relatively large discharge particles (of the order of hundreds of nm in size) seen on the DMSO cathodes, no large discharge products were noted for the cathodes discharged in nearly anhydrous (200 ppm H_2O) TEGDME. Discharge product formation was more apparent on cathodes containing PVDF. A higher magnification image is provided in Figure S2 which shows several very thin toroidal discharge products. In contrast, cathodes discharged galvanostatically within a higher H_2O content TEGDME electrolyte (1000 ppm H_2O) showed the formation of characteristic Li_2O_2 toroids as reported in a large number of previous reports (Figure S3).[8,22,26,48,70] The lack of large discharge products may explain the poor discharge capacities seen in Figure 1) and possibly also the severely limited

Downloaded on 2015-11-05 to IP 143.239.221.132 address. Redistribution subject to ECS terms of use (see ecsdl.org/site/terms_use) unless CC License in place (see abstract).

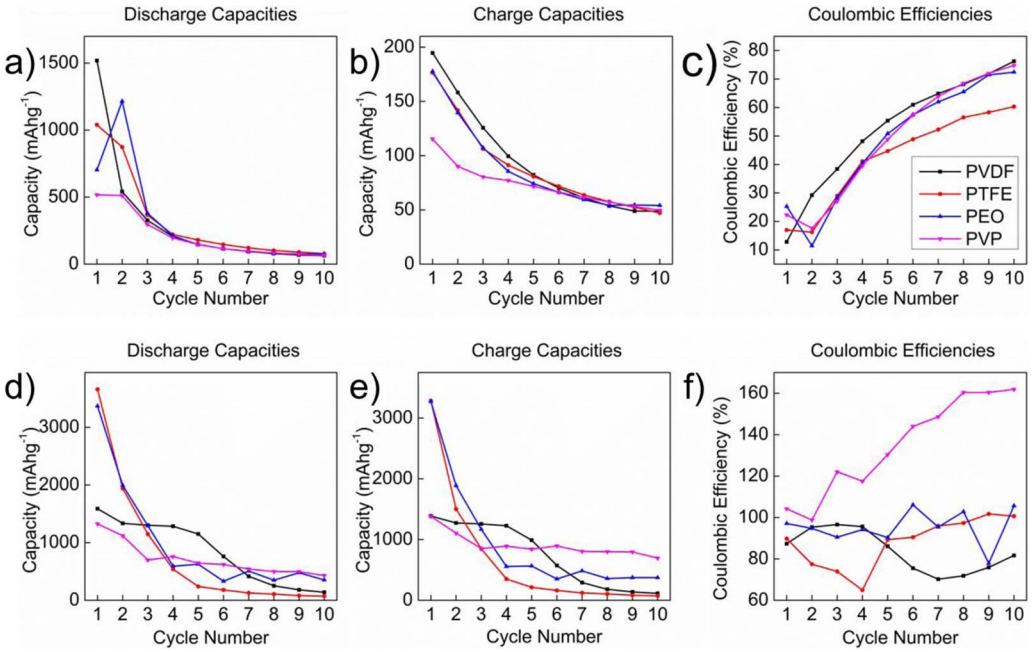

Figure 3. Discharge, charge and coulombic efficiency summaries for cycling data for the cathodes with different binders in TEGDME (a, b, c respectively) and DMSO (d, e, f respectively). In the cases where this value is over 100%, it means that the charge capacity is greater than the preceding discharge capacity, which strongly suggests side-reactions as a CE of 100% would suggest complete decomposition of the discharge products formed from the previous discharge.

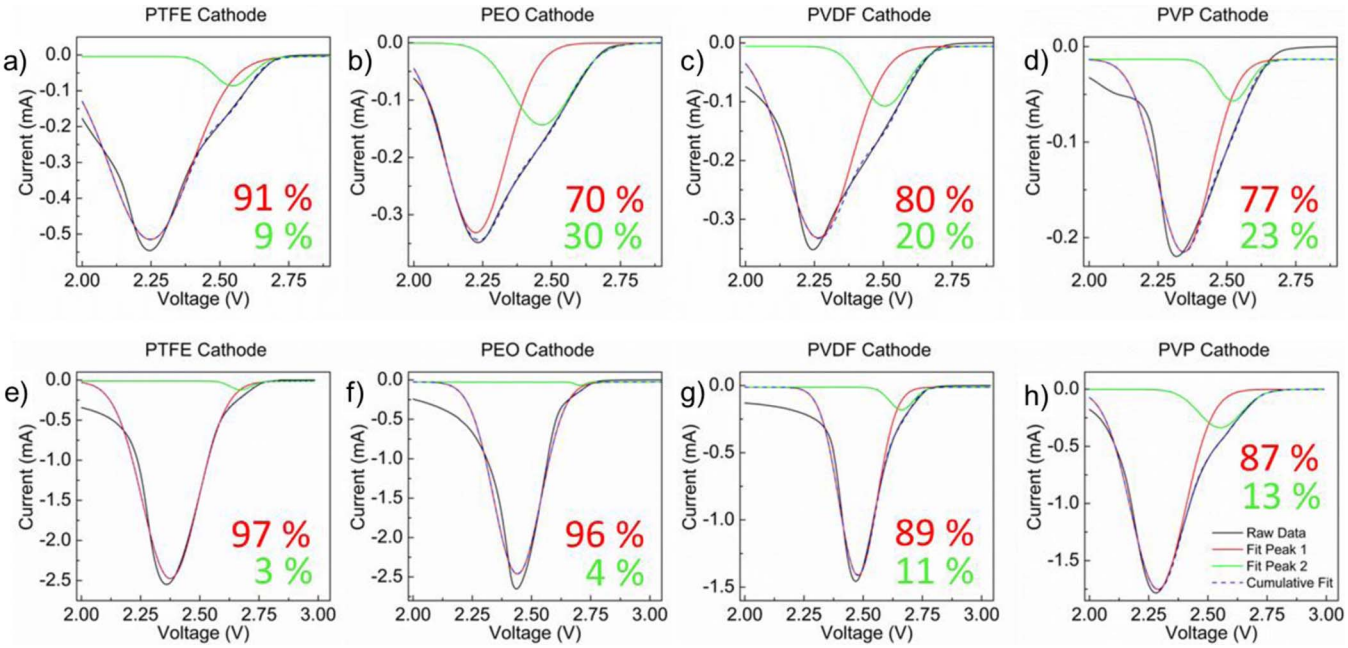

Figure 4. Comparison of linear voltage sweeps for the various cathode binders at a scan rate of 0.05 mV/s from OCV to 2 V. The tests using TEGDME and DMSO are shown in a)-d) and e)-h) respectively. The data is deconvoluted into solution (red curves) and surface (green curves) driven processes and their percentage contribution to the total raw data is given in each plot.

rechargeability. Given the insulating nature of Li_2O_2, it is possible that a thin conformal layer of Li_2O_2 on the surface may be passivating the cathode. Charging may be possible for these cathodes at higher potentials but the upper limit employed here (4.5 V) is already within the voltage range where parasitic side-reactions would be expected to occur.[17]

Ten discharge and charge cycles were also carried out on PEO based cathodes in an air atmosphere. Guo et al. have previously shown that the relative humidity of the air/O_2 used during battery operation strongly influences the electrochemical response.[71] The aim here was to compare the respective responses for DMSO and TEGDME based tests. While PEO can in no way be considered a fully 'stable' binder,[57] it is among the most commonly used binders in the literature and also behaved well in the above tests in TEGDME and DMSO in O_2. These tests were conducted to investigate the influence of CO_2 and H_2O contamination (which are known to have a large effect on the fundamental electrochemical processes occurring) on the electrochemical response for the cells.[14] The tests were performed with all parameters similar to test conducted in O_2, except that the O_2 inlet line was not connected and the cell was left open to air for the duration of the test. The relative

Downloaded on 2015-11-05 to IP 143.239.221.132 address. Redistribution subject to ECS terms of use (see ecsdl.org/site/terms_use) unless CC License in place (see abstract).

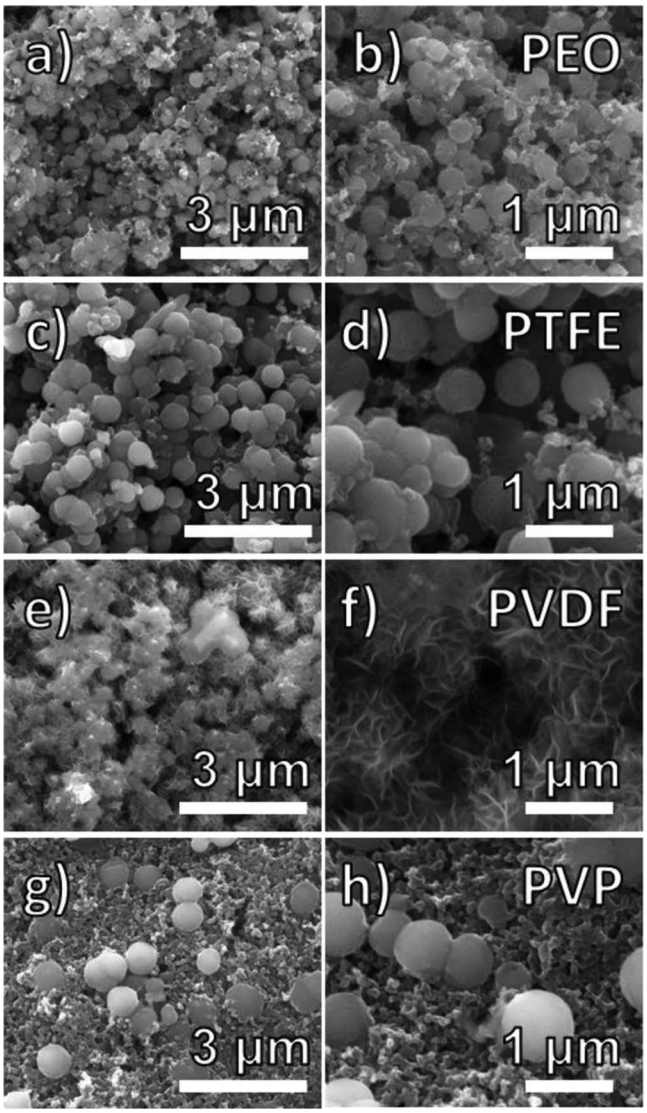

Figure 5. SEM images of Super P cathodes after the LVS shown in Figure 4 in the DMSO electrolyte for (a,b) PEO, (c,d) PTFE, (e,f) PVDF, (g,h) PVP.

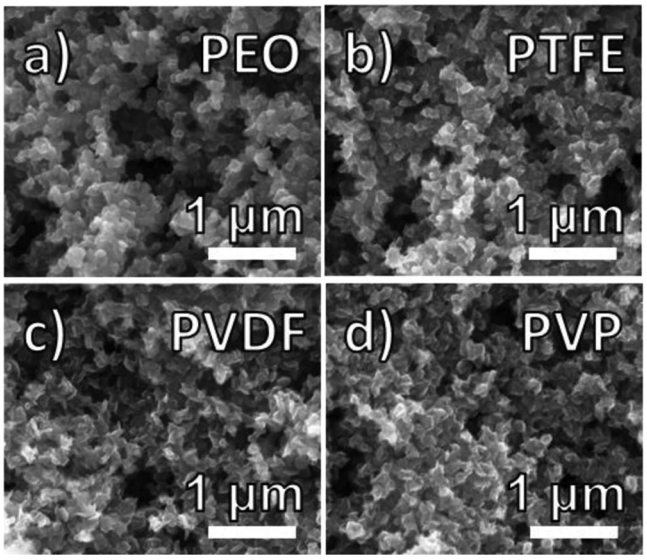

Figure 6. SEM images of Super P cathodes after the LVS shown in Figure 4 in the TEGDME electrolyte for (a,b) PEO, (c,d) PTFE, (e,f) PVDF, (g,h) PVP.

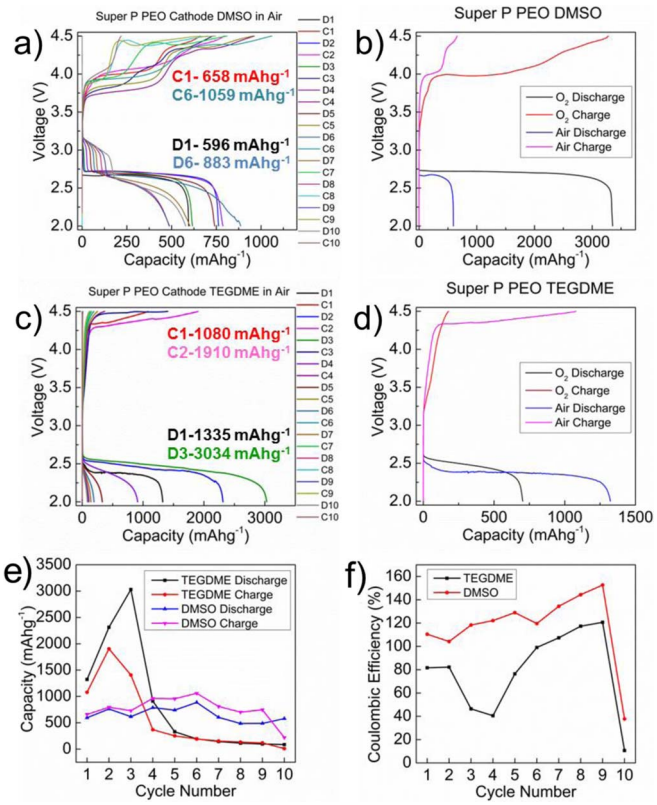

Figure 7. Galvanostatic tests conducted in air. a) 10 discharge and charge cycles of a Super P cathode with PEO binder discharged with a DMSO electrolyte in air. b) Comparison of the first discharge and charge profiles for DMSO electrolyte in air and O_2. c) 10 discharge and charge cycles of a Super P cathode with PEO binder discharged with a TEGDME electrolyte in air. d) Comparison of the first discharge and charge profiles for TEGDME electrolyte in air and O_2. e) Discharge and charge capacity summaries for the tests conducted in air and f) coulombic efficiencies. The values for the first and maximum discharge/charge capacities for the DMSO and TEGDME tests are included in a) and c) for clarity. Coulometric efficiencies >100% relate to a charge capacity greater than the preceding discharge capacity Li-air cells.

humidity in the laboratory was estimated at between 75–85% over the course of the test. The response for the cathode cycled in air using the DMSO electrolyte (Figure 7a) was markedly different to the cycling data presented previously in Figure 2. It should be noted that the discharge capacities did not decrease linearly with cycle number and the maximum discharge capacity was noted for the 6th discharge. From the 5th discharge, an additional higher voltage feature (seen at above 3 V in the discharge profiles) appears and increases in magnitude until the 10th cycle. To investigate the H_2O uptake of the electrolytes when in open air conditions, samples of the electrolyte were removed from the glove box and left in closed, air-filled containers for 24 h. The water content of the two electrolytes increased dramatically in just 24 h (well within the time frame of the galvanostatic tests run in air) up to 0.9% (from 0.02%) for the TEGDME electrolyte and 2.1% (from 0.01%) for DMSO.

The electrochemical responses for the first discharge and charges of the O_2 and air tests are compared in Figure 7b) for the DMSO electrolyte. The discharge and charge capacities were much lower for the tests run in air (595 mAhg^{-1} and 657 mAhg^{-1} respectively) than for the tests run in O_2 (3554 mAhg^{-1} and 3272 mAhg^{-1} respectively). In the case of the test run in DMSO, it was noted that the Li anode was completely white after the 10 discharge/charge cycles which may explain this peculiar discharge behavior. Given that the DMSO absorbs more water than the TEGDME electrolyte, corrosion of the Li anode is expected given the high reactivity of Li anodes with H_2O.[47] The Li

Downloaded on 2015-11-05 to IP 143.239.221.132 address. Redistribution subject to ECS terms of use (see ecsdl.org/site/terms_use) unless CC License in place (see abstract).

foil in the case of the TEGDME electrolyte was not corroded and was still shiny after the test. Reactions occurring at the Li anode surface have not been widely studied/ reported (as a function of electrolyte type, water content, cathode composition etc.) for the Li-O_2 systems and require further study.[72] The initial discharge potential for the first discharge in air was 2.67 V, which is slightly lower than the 2.73 V noted for the test run in O_2. The onset of charging for the test in air occurs slightly below 4 V which is similar to the voltage seen for the test in O_2, however, significantly more charging occurs in subsequent cycles between 3.5 V and 4 V with the largest charge capacity seen for the 6th charge. These additional 'charging' responses are almost certainly due to parasitic side-reactions and are not noted for the tests which use pure O_2. However, these lower potential features are certainly of interest given the large number of Li-O_2 reports which assign electrocatalysis based solely on a lowering of charge potential.

Similarly, for the galvanostatic tests run in TEGDME (Figure 7c), the first discharge capacity was lower than the second and third discharge cycles (suggesting an increased discharge capacity with cycling due to the increasing H_2O content in the electrolyte over time). Interestingly, there was significantly better charging noticed for cells containing TEGDME conducted in air compared to the corresponding TEGMDE test in a closed O_2 environment. This may have been due to the formation of a more easily decomposed Li_2O_2 morphology (i.e. toroids), increased side reactions due to the presence of H_2O/CO_2, or a combination of both effects. The increase in the amount of charging behavior and increased discharge capacities are clearly seen in Figure 7d) where the first discharge charge profiles are compared for the tests run in air and O_2. The discharge and charge capacities for each of the tests are presented in Figure 7e and show that the initial increase in discharge capacity is particularly large for the test in TEGDME. The coulombic efficiencies for the DMSO test (Figure 7f) are all above 100% apart from the 10th cycle where a marked drop-off (likely associated with cell death) was seen. This value of coulombic efficiency reflects the complex discharge/charge electrochemistry occurring in air for the DMSO electrolyte and likely reflects extensive side-reactions.

Conclusions

In conclusion, the influence of electrode binder and electrolyte solvent on the electrochemical response of carbon based Li-O_2 cathodes has been investigated. The electrochemical performances of carbon cathodes containing different binders (PTFE, PVDF, PVP and PEO) were contrasted in two different electrolytes (nearly anhydrous TEGDME and DMSO). The discharge capacities and rechargeability were noticeably different between the two electrolyte systems. Nearly anhydrous TEGDME showed extremely poor rechargeability in the voltage range of 2–4.5 V. In contrast, DMSO electrolyte tested cathodes showed better rechargeability and much higher discharge capacities. Through the use of LSV, it was shown that the binder constituent can directly influence the fundamental electrochemical response for discharge with a marked difference (ORR potential) for the various samples discharged voltammetrically in DMSO. SEM analysis of cathodes showed the formation of large particles (assumed to be Li_2O_2) for three of the four binders discharged in DMSO. The size of the particles formed was linked to the ORR onset potential. In the case of PVDF cathodes, large flaky discharge products were noted which were characteristic of LiOH and thus highlight the prevalence of side-reactions even in short dwell time experiments.

In contrast, LSV of the different carbon cathodes in a nearly anhydrous TEGDME electrolyte showed lower current values and smaller differences in the ORR voltage. Unlike previous reports (including our own work) using ethereal electrolyte solvents, toroidal formation of Li_2O_2 was not readily identified with only PVDF cathodes showing any indication of obvious Li_2O_2 formation (as thin disks). The lack of toroids in these tests was ascribed to the low water content of the electrolyte and also used to rationalize the poor discharge capacities. Galvanostatic experiments were also conducted for PEO cathodes in air (rather than O_2) to investigate the influence of ambient H_2O and CO_2 on the electrochemical response. Control experiments showed a considerable increase in H_2O content in the electrolytes in a 24 period from 100 and 200 ppm to ≈2% (20,000 ppm) and ≈0.9% (9,000 ppm) for DMSO and TEGDME respectively. Tests run in air for the DMSO electrolyte showed the emergence of lower overpotential features on both the discharge and charge profiles while the discharge capacity and apparent rechargeability was improved for TEGDME. The report highlights the importance of using sophisticated analytical tools (beyond qualitative techniques such as XRD) for the verification of genuine electrocatalysis and also further highlights the importance of compatible electrolyte and binder pairings in identifying more stable Li-O_2 battery components.

Acknowledgments

This research has received funding from the Seventh Framework Programme FP7/2007-2013 (Project STABLE) under grant agreement no. 314508. This work was also supported by Science Foundation Ireland (SFI) through an SFI Technology Innovation and Development Award under contract no. 13/TIDA/E2761. Support from the Irish Research Council New Foundations Award is gratefully acknowledged.

References

1. P. G. Bruce, S. A. Freunberger, L. J. Hardwick, and J. M. Tarascon, *Nat. Mater.*, **11**, 19 (2011).
2. P. G. Bruce, L. J. Hardwick, and K. Abraham, *MRS Bull.*, **36**, 506 (2011).
3. G. Girishkumar, B. McCloskey, A. C. Luntz, S. Swanson, and W. Wilcke, *J. Phys. Chem. Lett.*, **1**, 2193 (2010).
4. M. D. Bhatt, H. Geaney, M. Nolan, and C. O'Dwyer, *Phys. Chem. Chem. Phys.*, **16**, 12093 (2014).
5. K. Abraham and Z. Jiang, *J. Electrochem. Soc.*, **143**, 1 (1996).
6. C. O. Laoire, S. Mukerjee, K. M. Abraham, E. J. Plichta, and M. A. Hendrickson, *J. Phys. Chem. C*, **113**, 20127 (2009).
7. Y.-C. Lu, D. G. Kwabi, K. P. C. Yao, J. R. Harding, J. Zhou, L. Zuin, and Y. Shao-Horn, *Energy Environ. Sci.*, **4**, 2999 (2011).
8. R. Black, J.-H. Lee, B. Adams, C. A. Mims, and L. F. Nazar, *Angew. Chem. Int. Edn.*, **52**, 392 (2013).
9. Z. Peng, S. A. Freunberger, Y. Chen, and P. G. Bruce, *Science*, **337**, 563 (2012).
10. M. M. O. Thotiyl, S. A. Freunberger, Z. Peng, Y. Chen, Z. Liu, and P. G. Bruce, *Nat. Mater.* **12**, 1050, (2013).
11. B. M. Gallant, D. G. Kwabi, R. R. Mitchell, J. Zhou, C. Thompson, and Y. Shao-Horn, *Energy Environ. Sci.* **6**, 2518 (2013).
12. B. Horstmann, B. Gallant, R. Mitchell, W. G. Bessler, Y. Shao-Horn, and M. Z. Bazant, *J. Phys. Chem. Lett.*, **4**(24), 4217 (2013).
13. B. D. McCloskey, A. Valery, A. C. Luntz, S. R. Gowda, G. M. Wallraff, J. M. Garcia, T. Mori, and L. E. Krupp, *J. Phys. Chem. Lett.*, **4**(17), 2989 (2013).
14. S. R. Gowda, A. Brunet, G. M. Wallraff, and B. D. McCloskey, *J. Phys. Chem. Lett.*, **4**(2), 276 (2012).
15. H.-K. Lim, H.-D. Lim, K.-Y. Park, D.-H. Seo, H. Gwon, J. Hong, W. A. Goddard III, H. Kim, and K. Kang, *J. Am. Chem. Soc.*, **135**, 9733 (2013).
16. B. D. McCloskey, A. Speidel, R. Scheffler, D. C. Miller, V. Viswanathan, J. S. Hummelshøj, J. K. Nørskov, and A. C. Luntz, *J. Phys. Chem. Lett.*, **3**, 997 (2012).
17. M. M. Ottakam Thotiyl, S. A. Freunberger, Z. Peng, and P. G. Bruce, *J. Am. Chem. Soc.*, **135**(1), 494 (2012).
18. Y. Hu, X. Han, F. Cheng, Q. Zhao, Z. Hu, and J. Chen, *Nanoscale*, **6**, 177 (2014).
19. D. Zhai, H.-H. Wang, J. Yang, K. C. Lau, K. Li, K. Amine, and L. A. Curtiss, *J. Am. Chem. Soc.*, **135**, 15364 (2013).
20. E. Yilmaz, C. Yogi, K. Yamanaka, T. Ohta, and H. R. Byon, *Nano Lett.*, **13**, 4679 (2013).
21. N. B. Aetukuri, B. D. McCloskey, J. M. García, L. E. Krupp, V. Viswanathan, and A. C. Luntz, *arXiv preprint arXiv:1406.3335* (2014).
22. W. Fan, Z. Cui, and X. Guo, *J. Phys. Chem. C*, **117**(6), 2623 (2013).
23. D. Xu, Z. L. Wang, J. J. Xu, L. L. Zhang, L. M. Wang, and X. B. Zhang, *Chem. Commun.*,**48**, 11674 (2012).
24. J.-H. Lee, R. Black, G. Popov, E. Pomerantseva, F. Nan, G. A. Botton, and L. F. Nazar, *Energy Environ. Sci.*, **5**, 9558 (2012).
25. H. Geaney, J. O'Connell, J. D. Holmes, and C. O'Dwyer, *J. Electrochem. Soc.*, **161**, A1964 (2014).
26. B. D. Adams, C. Radtke, R. Black, M. L. Trudeau, K. Zaghib, and L. F. Nazar, *Energy Environ. Sci.*, **6**, 1772 (2013).
27. M. H. Cho, J. Trottie, C. Gagnon, P. Hovington, D. Clément, A. Vijh, C. S. Kim, A. Guerfi, R. Black, L. Nazar, and K. Zaghib, *J. Power Sources.*, **268**, 565 (2014).
28. A. Khetan, A. Luntz, and V. Viswanathan, *J. Phys. Chem. Lett.*, **6**, 1254 (2015).
29. L. Johnson, C. Li, Z. Liu, Y. Chen, S. A. Freunberger, P. C. Ashok, B. B. Praveen, K. Dholakia, J.-M. Tarascon, and P. G. Bruce, *Nat. Chem.*, **6**, 1091 (2014).

Downloaded on 2015-11-05 to IP 143.239.221.132 address. Redistribution subject to ECS terms of use (see ecsdl.org/site/terms_use) unless CC License in place (see abstract).

30. B. D. McCloskey, D. S. Bethune, R. M. Shelby, G. Girishkumar, and A. C. Luntz, *J. Phys. Chem. Lett.*, **2**, 1161 (2011).
31. M. Balaish, A. Kraytsberg, and Y. Ein-Eli, *Phys. Chem. Chem. Phys.*, **16**, 2801 (2014).
32. F. Mizuno, S. Nakanishi, Y. Kotani, S. Yokoishi, and H. Iba, *Electrochemistry*, **78**, 403 (2010).
33. J. Read, *J. Electrochem. Soc.*, **153**, A96 (2006).
34. S. A. Freunberger, Y. Chen, N. E. Drewett, L. J. Hardwick, F. Bardé, and P. G. Bruce, *Angew. Chem. Int. Edn.*, **50**, 8609 (2011).
35. K. R. Ryan, L. Trahey, B. J. Ingram, and A. K. Burrell, *J. Phys. Chem. C*, **116**, 19724 (2012).
36. D. Xu, Z.-l. Wang, J.-j. Xu, L.-l. Zhang, and X.-b. Zhang, *Chem. Commun.*, **48**, 6948 (2012).
37. M. J. Trahan, S. Mukerjee, E. J. Plichta, M. A. Hendrickson, and K. Abraham, *J. Electrochem. Soc.*, **160**, A259 (2013).
38. D. G. Kwabi, T. P. Batcho, C. V. Amanchukwu, N. Ortiz-Vitoriano, P. Hammond, C. V. Thompson, and Y. Shao-Horn, *J. Phys. Chem. Lett.*, **5**(16), 2850 (2014).
39. R. Younesi, P. Norby, and T. Vegge, *ECS Electrochem. Lett.*, **3**, A15 (2014).
40. E. J. Nemanick and R. P. Hickey, *J. Power Sources*, **252**, 248 (2014).
41. X.-H. Yang and Y.-Y. Xia, *J. Solid State Electrochem.*, **14**, 109 (2010).
42. M. Song, D. Zhu, L. Zhang, X. Wang, R. Mi, H. Liu, J. Mei, L. W. Lau, and Y. Chen, *J. Solid State Electrochem.*, **18**, 739 (2014).
43. M. Song, D. Zhu, L. Zhang, X. Wang, L. Huang, Q. Shi, R. Mi, H. Liu, J. Mei, and L. W. Lau, *J. Solid State Electrochem.*, **17**, 2061 (2013).
44. J.-B. Park, J. Hassoun, H.-G. Jung, H.-S. Kim, C. S. Yoon, I. Oh, B. Scrosati, and Y.-K. Sun, *Nano Lett.*, **13**(6), 2971 (2013).
45. K. U. Schwenke, M. Metzger, T. Restle, M. Piana, and H. A. Gasteiger, *J. Electrochem. Soc.*, **162**, A573 (2015).
46. H. Geaney and C. O'Dwyer, *Phys. Chem. Chem. Phys.*, **17**, 6748 (2015).
47. S. Meini, M. Piana, N. Tsiouvaras, A. Garsuch, and H. A. Gasteiger, *Electrochem. Solid-State Lett.*, **15**, A45 (2012).
48. N. B. Aetukuri, B. D. McCloskey, J. M. García, L. E. Krupp, V. Viswanathan, and A. C. Luntz, *Nat. Chem.*, **7**, 50 (2015).
49. E. Nasybulin, W. Xu, M. H. Engelhard, Z. Nie, S. D. Burton, L. Cosimbescu, M. E. Gross, and J.-G. Zhang, *J. Phys. Chem. C*, **117**(6), 2635 (2013).
50. G. M. Veith, J. Nanda, L. H. Delmau, and N. J. Dudney, *J. Phys. Chem. Lett.*, **3**, 1242 (2012).
51. F. Li, S. Wu, T. Zhang, P. He, A. Yamada, and H. Zhou, *Nat. Commun.*, **6**, 7843 (2015).
52. D. Sharon, D. Hirsberg, M. Afri, F. Chesneau, R. Lavi, A. A. Frimer, Y.-K. Sun, and D. Aurbach, *ACS Appl. Mater. Interfaces*, **7**(30), 16590 (2015).
53. Y. Zhang, H. Zhang, J. Li, M. Wang, H. Nie, and F. Zhang, *J. Power Sources*, **240**, 390 (2013).
54. G. A. Elia, J.-B. Park, B. Scrosati, Y.-K. Sun, and J. Hassoun, *Electrochem. Commun.*, **34**, 250 (2013).
55. Y. Wang and H. Zhou, *Energy Environ. Sci.*, **4**, 1704 (2011).
56. N. Ding, S. Chien, T. S. A. Hor, R. Lum, Y. Zong, and Z. Liu, *J. Mater. Chem. A*, **2**, 12433 (2014).
57. J. R. Harding, C. V. Amanchukwu, P. T. Hammond, and Y. Shao-Horn, *J. Phys. Chem. C*, **119**(13), 6947 (2015).
58. C. V. Amanchukwu, J. R. Harding, Y. Shao-Horn, and P. T. Hammond, *Chem. Mater.*, **27**(2), 550 (2015).
59. R. Black, S. H. Oh, J.-H. Lee, T. Yim, B. Adams, and L. F. Nazar, *J. Am. Chem. Soc.*, **134**, 2902 (2012).
60. B. D. McCloskey, R. Scheffler, A. Speidel, D. S. Bethune, R. M. Shelby, and A. C. Luntz, *J. Am. Chem. Soc.*, **133**, 18038 (2011).
61. R. Cao, J.-S. Lee, M. Liu, and J. Cho, *Adv. Energy Mater.*, **2**, 816 (2012).
62. S. H. Oh and L. F. Nazar, *Adv. Energy Mater.*, **2**, 903 (2012).
63. B. Sun, X. Huang, S. Chen, P. Munroe, and G. Wang, *Nano Lett.*, **14**, (6), 3145 (2014).
64. S. Beattie, D. Manolescu, and S. Blair, *J. Electrochem. Soc.*, **156**, A44 (2009).
65. N. Tsiouvaras, S. Meini, I. Buchberger, and H. Gasteiger, *J. Electrochem. Soc.*, **160**, A471 (2013).
66. A. C. Luntz and B. D. McCloskey, *Chem. Rev.*, **114**(23), 11721 (2014).
67. S. R. Younesi, S. Urbonaite, F. Björefors, and K. Edström, *J. Power Sources*, **196**, 9835 (2011).
68. L. Nazar, D. Kundu, R. Black, and E. Jamstorp, *Energy Environ. Sci.* **8**, 1292 (2015).
69. J. Lu, Y. Lei, K. C. Lau, X. Luo, P. Du, J. Wen, R. S. Assary, U. Das, D. J. Miller, and J. W. Elam, *Nat. Commun.*, **4**, 2383 (2013).
70. S. H. Oh, R. Black, E. Pomerantseva, J.-H. Lee, and L. F. Nazar, *Nat. Chem.*, **4**, 1004 (2012).
71. Z. Guo, X. Dong, S. Yuan, Y. Wang, and Y. Xia, *J. Power Sources*, **264**, 1 (2014).
72. J.-L. Shui, J. S. Okasinski, P. Kenesei, H. A. Dobbs, D. Zhao, J. D. Almer, and D.-J. Liu, *Nat. Commun.*, **4**, 2255 (2013).

Downloaded on 2015-11-05 to IP **143.239.221.132** address. Redistribution subject to ECS terms of use (see **ecsdl.org/site/terms_use**) unless CC License in place (see abstract).